Applied Thermal Engineering 176 (2020) 115430

Contents lists available at ScienceDirect

Applied Thermal Engineering

journal homepage: www.elsevier.com/locate/apthermeng

Lateral dispersion in a lattice porous heater core for compact operations

Taahir I. Bhaiyat[a,c], Tian Jian Lu[b,c], Tongbeum Kim[a,b,c,*]

[a] School of Mechanical and Aeronautical Engineering, University of the Witwatersrand, Johannesburg 2000, South Africa
[b] State Key Laboratory of Mechanics and Control of Mechanical Structures, Nanjing University of Aeronautics and Astronautics, Nanjing 210016, PR China
[c] Nanjing Center for Multifunctional Lightweight Materials and Structures, Nanjing University of Aeronautics and Astronautics, Nanjing 210016, PR China

HIGHLIGHTS

- Non-uniform incident flows reduce thermal performance of conventional heater cores.
- A lattice porous core promotes lateral dispersion of non-uniform incident flows.
- Lateral dispersion enhances thermal performance.
- Increased lateral dispersion occurs under non-uniform incident flows.

ARTICLE INFO

Keywords:
Automotive climate control systems
Compact heat exchangers
Lattice porous core
Lateral dispersion
Louvered fins

ABSTRACT

Louvered fin-and-tube cores have been the most popular choice for enhancing the heat transfer performance of compact heat exchangers such as automotive climate control systems (ACCS), because of their moderate heat removal capacity with least pressure drop compared to other heat exchanger core elements. However, their performance in such systems is debilitated if the incident coolant stream is highly non-uniform due to lateral blockage of flow by the fins resulting from compactness of the overall system. This study demonstrates how such lateral blockage imposed by a conventional louvered fin-and-tube core can be relieved by a "lattice porous core" which induces three-dimensional momentum/thermal dispersion within the core under non-uniform incident coolant streams. Especially under the highly localized non-uniform distribution of coolant streams found in a typical ACCS, the lattice porous core thermally outperforms the conventional core by up to 35% within its typical operational range.

1. Introduction

An automotive climate control system (ACCS) adjusts air properties such as humidity and temperature in a cabin of ground vehicles. To heat up an ambient air-stream before entering the passenger cabin, the ACCS makes use of compact finned tube heat exchanger cores wherein the forced air stream is passed over external (finned) surfaces of regularly arranged tubes with hot liquid flowing inside them (Fig. 1). Thus, heat is transferred by forced convection from the liquid-stream to the air-stream across the thin tube walls, and consequently the temperature of the air-stream is raised.

A practical method of augmenting the heat transfer rate is to modify the fins so that the air-stream's mixing and/or wall shear stress characteristics are passively enhanced. In this connection, periodic surface interruptions such as perforations, offset strips, or louvers are commonly found on the fin surfaces of virtually all compact heat exchanger cores. Such interruptions, however, typically result in increased form drag (i.e., drag induced by a low-pressure region formed in the separated flow, or wake, downstream of an interruption). Kays & London [1] and Jacobi & Shah [2] have reported on the heat transfer and flow friction characteristics of several interrupted fin surfaces. Their studies concluded that, compared to other types of interrupted fins (e.g., wavy fins, offset-strip fins, and perforated fins), louvered fins (Fig. 2(a,b)) provide a moderate heat transfer performance with a relatively low pressure drop penalty.

Therefore, the thermo-fluidic aspects of such louvered fins have been studied extensively, with several correlations reported in the open literature for operation under uniform air streams [3–8]. It is understood that increased heat transfer and pressure drop are associated with the increase in the velocity component of the air-streams parallel to the louvers (commonly referred to as "louver-directed flow") as shown in Fig. 2(c). This is because when air flows along the thin louver surfaces,

* Corresponding author.
E-mail address: tongbeum.kim@nuaa.edu.cn (T. Kim).

https://doi.org/10.1016/j.applthermaleng.2020.115430
Received 28 January 2020; Received in revised form 28 April 2020; Accepted 30 April 2020
Available online 11 May 2020
1359-4311/

Nomenclature

A_a	total air-side heat transfer surface area [m^2]
A_w	total water-side heat transfer surface area [m^2]
A_t	tube wall conduction area [m^2]
b	fin height [mm]
C	heat capacity rate [W/K]
C_r	heat capacity rate ratio [–]
c_p	specific heat capacity [J/kg-K]
δ	fin thickness [mm]
D	diameter [mm]
D_h	hydraulic diameter of the rectangular cooling channel [mm]
d	turbine meter diameter [mm]
η_o	surface efficiency [–]
η_f	fin efficiency [–]
ε	effectiveness [–]
h	heat transfer coefficient [W/m^2-K]
H	core height [mm]
H_t	flat tube height [mm]
j	Colburn j-factor [–]
k	thermal conductivity [W/m-K]
l_p	Louver pitch [mm]
l_h	Louver height [mm]
l_l	fin ligament length [mm]
L_t	tube depth [mm]
L_f	fin depth [mm]
$\dot{m}$	mass flow rate [kg/s]
NTU	number of transfer units [–]
Nu	Nusselt number [–]
Pr	Prandtl number [–]
P_f	fin pitch [mm]
$\dot{q}$	heat transfer rate [W]
Q	flow rate [litre/s]
ρ	density [kg/m^3]
Re	Reynolds number [–]
R	overall thermal performance ratio [–]
R_f	fins thermal performance ratio [–]
r	tube rib thickness [mm]
S_T	transverse tube pitch [mm]
S_L	longitudinal tube pitch [mm]
S_1	deflection louver length [mm]
S_2	turnaround louver length [mm]
θ	Louver angle [°]
t	flat tube wall thickness [mm]
T	temperature [K]
u	local fluid velocity [m/s]
u_m	mean fluid velocity [m/s]
U	overall heat transfer coefficient [W/m^2-K]
W	core width [mm]

Subscripts

a	air
al	aluminum
h	hydraulic
in	inlet
i	inner
l	ligament
min	minimum
max	maximum
Out	outlet
o	outer
t	tube
w	water

periodic destruction and growth of the boundary layer occur with a thin wake downstream of each louver. For such a flow system to be prevalent, it is generally required that the ratio of fin pitch to louver pitch (P_f/l_p as denoted in Fig. 2(c)) is small to minimize hydraulic resistance in the preferred (louver-directed) path. Additionally, this preferred path requires a sufficiently large Reynolds number such that boundary layer growth over the louver surfaces does not block off the fresh mainstream from entering the louver passages [9]. Otherwise, air-streams parallel to the fins prevail and thick uninterrupted boundary layers persist, resulting in a duct-like flow with relatively lower heat transfer performance, commonly referred to as “duct-directed” flow [5,8].

The thermo-fluidic performance of louvered-fin cores is generally well established for uniform, unidirectional air streams perpendicular to the core and without any disturbances or flow area changes upstream and downstream of the core (referred to as “design conditions” throughout this study). Less clearly understood phenomena in contemporary literature seem to be associated with the performance of these cores under “off-design” conditions. This refers to the actual flow conditions typically encountered in compact heat exchanger applications, such as macro-scale non-uniformity of the air-streams upstream of the core. This off-design condition has particularly been given attention by researchers [10–12], who have reported as much as 30% overall heat transfer deterioration. However, the physical mechanisms responsible for this deterioration are still poorly understood.

Blecich [12] alluded to favourable orientations between the air-stream’s velocity gradient and the fin plane, reporting that the degree of air redistribution by a straight finned core contributed to the core’s overall thermal performance. The author mentioned that the redistribution characteristics of a core may be affected by fin interruptions, such as slits or louvers, but this was not explicitly quantified. With only two possible flow paths through a typical louvered fin (i.e., duct- or louver-directed), a louvered-fin core has been shown to have limited capability to disperse (i.e., to spread out, or re-distribute) an incidentally non-uniform air-stream. In this connection, flow visualization studies [9,13–14] suggest that a streamline from an inlet deflection louver retreats the corresponding exit louver (on the same fin), regardless of whether the flow is duct- or louver-directed. As a result, the maximum heat transfer surface area of the core becomes compromised. This is because local concentrations of momentum in an incidentally non-uniform flow-stream are unable to spread to different regions of the core once the flow-stream enters the fin passages. In addition, louvered fins do not perform optimally at low Reynolds numbers (i.e., when duct-directed flow is prevalent) [3,9]. Thus, where the local flow velocity is low, there is a local deterioration in heat transfer due to thicker boundary layers on the fin surface. Bhaiyat et al. [15] concluded that this limitation severely reduces the thermal performance of a louvered fin-and-tube core when operated under certain off-design conditions particular to ACCS units.

The overall heat transfer performance of louvered fin-tube cores is thought to be sensitive to local distortions of the inlet velocity distribution, since they are inherently unable to disperse a local flow-stream. Yet the flow-stream upstream of the heater core in a typical automotive climate control system (ACCS) is usually non-uniform, due to the unit’s compact geometry [11,15]. In fact, the incident streams to several other heat exchangers also tend to be non-uniform, inclined, and/or poorly distributed for the sake of compactness of the overall systems [16,17]. Such undesired flow distributions can typically be overcome with specially designed intakes or headers, which ideally distribute the flow-stream before it enters a fluidic device [18,19]. In an ACCS unit, however, there is no space for additional upstream

components; compact fin-and-tube heater cores inevitably operate under a non-uniform incident flow, with sub-optimal thermal performance.

The scarcity of data supporting the fluidic mechanisms responsible for the thermal performance deterioration of compact cores at off-design conditions presumably dissuades their ground-up design for ACCS units. This study, however, squarely addresses the physical mechanism behind the reported thermal performance deteriorations. Based on the findings, a newly designed compact core is shown to mitigate the adverse effects of non-uniform flow on the overall thermal performance of a core. In particular, a "lattice porous core" with specially arranged longitudinal and transverse circular ligaments that function respectively as tubes (i.e., hollow circular tubes) and fins (i.e., solid circular rods) provides suitable aerodynamic anisotropy [20] to facilitate lateral dispersion of the air-stream within the core. To demonstrate its effectiveness in enhancing the heat transfer performance of an ACCS requiring a certain compact operation (e.g., a highly non-uniform incident coolant stream), a series of experiments and design iterations have been performed to address the following issues. Firstly, the lattice porous core's ability to re-distribute a non-uniform incident air-stream was assessed relative to a conventional louvered fin-and-tube core. Secondly, the heat transfer performance of both the louvered fin-and-tube and lattice porous cores under uniform and non-uniform incident streams were measured experimentally. This confirmed a possible mechanism for the reported heat transfer deteriorations in the louvered fin-and-tube cores under non-uniform incident flow-streams. Finally, the contribution of louvered and circular fins to the overall heat transfer performance of a given core was discussed, providing insights into enhanced thermal dispersion characteristics of the lattice porous heater core.

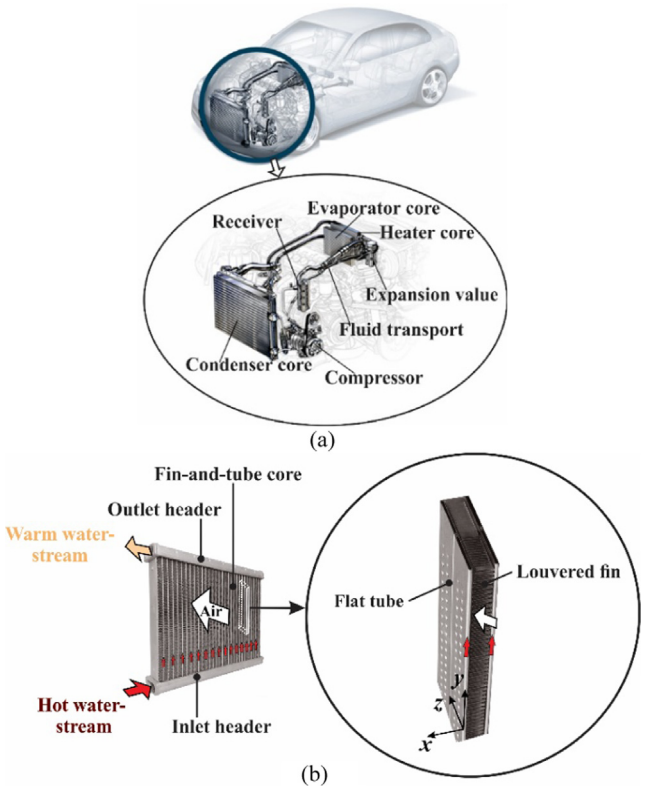

Fig. 1. Automotive climate control system: (a) Overall flow routes for internal and external working fluids in an automotive climate control system (ACCS) [21] (b) Typical heater core operation.

2. Experiments

2.1. Test rig and setup

A heater core was furnished with a closed-loop hot water supply system, shown schematically in Fig. 3(a), and placed inside a custom-built wind-tunnel shown in Fig. 3(b). A 12 V brushless DC pump circulates water through a plurality of electrical heaters, as well as through the test core. The water-side flowrate (Q_w) was monitored by a hall-effect sensor placed downstream of the exit header. Each electrical heater (with maximum power rating indicated in Fig. 3(a) was connected to an independent voltage regulator to adjust the electrical power input. Similar to the method adopted by Shinde [22], a 2 kW urn heater was installed to provide a backup heating system during testing and to minimize variations of the inlet water temperature, maintained at a constant temperature $T_{w,in}$. Using this approach, the experimental setup was capable of maintaining temperature variations less than 0.5 °C within the range of air volume flowrates tested. A 2.4 kW centrifugal fan capable of providing volume flowrates $0 \leq Q_a \leq 90$ L/s blows air at ambient temperature $T_{a,in}$ through a circular tube that is connected to a turbine flowmeter (Airflow^{TM}, UK (LCA501)). Downstream of which, a long rectangular flow developing section (width, $W = 47.6$ mm and height, $H = 160$ mm) with its length of 10 times the turbine's rotor diameter (d), was attached. Inside the channel, a honeycomb layer was positioned at $2d$ downstream from the inlet of the flow developing section. The test heater core of width (W) and height (H) was attached to the end of the rectangular flow channel of the same dimensions ($W \times H$) as shown in Fig. 3(b). At the outlet side of the core, another short rectangular channel was placed to avoid a sudden expansion of the air-stream that leaves the heater core.

In investigating non-uniform streams (i.e., the off-design configuration), the wind-tunnel of Fig. 3(b) was modified near the test section to simulate the inlet flow found in a typical ACCS unit. Based on the geometry of a commercial ACCS, a right-angled wedge with height $0.625H$, apex angle of 26.6°, and width W was fabricated and inserted immediately upstream of the heater core, (in Fig. 4(b) as opposed to the design condition in Fig. 4(a)). Downstream of the heater core, there were no further obstructions. The effect of any flow area contractions or expansions upstream of the heater core, as present in the ACCS were understood to have a negligible effect on the performance and not considered in this study [23].

2.2. Test cores

Four cores were tested in this study, whose geometries are given in Fig. 5. The dimensions of each tube, fin, and ligament are detailed in Table 1. Each of the flat tubes (in Fig. 5(a,b)), arranged transverse to the convective stream, have a cross sectional internal flow area of $A_c = 20.8$ mm^2 and an external surface area of $A_s = 8419$ mm^2 whereas each of the circular tube rows (in Fig. 5(c,d)), consisting of 5 tubes in the flow direction have a total internal cross sectional area of $A_c = 18.0$ mm^2 (approximately 10% smaller water flow area than the flat tubes) and an external surface area of $A_s = 7490$ mm^2. Both the flat and circular tubes are of equal lengths $L = 160$ mm.

The louvered fins and flat tubes were manufactured using conventional aluminium sheet metal having thermal conductivity $k_{al} \sim 205$ W/m-K (Hanon Systems, South Korea), while the circular tube bank and staggered fin ligaments were manufactured by additive laser sintering (Renishaw plc, UK) using AlSi10Mg whose thermal conductivity is, on average, given as $k_{al} \sim 160$ W/m-K.

2.3. Flow measurements

To determine the change in flow distribution caused by a given core, time-averaged velocity profiles were measured using a Pitot tube (KIMO, L-type, 3 mm diameter) placed at 0.75 times the tube depth

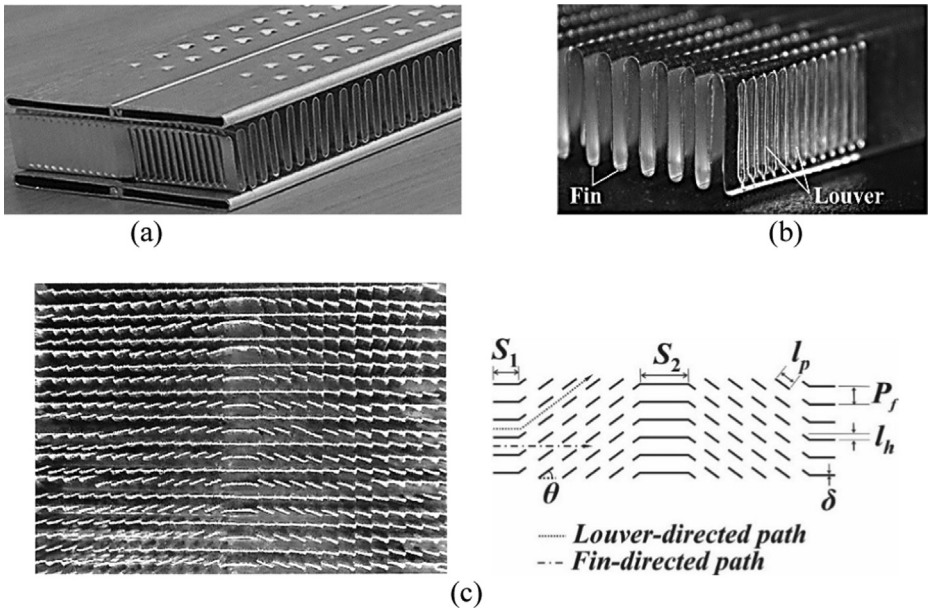

Fig. 2. Typical louvered fin and tube configuration in an ACCS heater core: (a) Fins sandwiched between flat tubes, (b) Louvers on the fin surfaces, (c) Cut-away view of the louvered fins and schematic representation of the louvered fin geometry.

(i.e., $0.75L_t$) downstream of each core as shown in Fig. 6. Two pressure ports of the Pitot tube were connected to a digital micro-manometer (TSI 9565). The wedge was placed immediately upstream of the core, blocking off the lower region (i.e., $0 \leq y/H \leq 0.4$). The Pitot tube was traversed from $y = 0$ to $y = H$ along the span-wise centerline of the wind-tunnel with increments of 0.5 cm.

2.4. Thermal measurements

For each core, having hot water fed through at a constant water-side Reynolds number $Re_w \approx 1000$ (based on the respective tube's internal hydraulic diameter) and constant water inlet temperature $T_{w,in} = 55$ °C, the exit temperature of the water-stream, $T_{w,out}$, and the inlet temperature of the air-stream, $T_{a,in}$, were recorded at steady-state for various air-stream flowrates, which were varied systematically in the range $30 < Q_a < 90$ L/s. The air-stream temperature ($T_{a,in}$) was measured using a T-type thermocouple $4L_t$ upstream of the heater core. The bulk mean water temperatures ($T_{w,in}$, $T_{w,out}$) were measured using T-type thermocouples placed $4.5L_t$ upstream of the inlet header and $4.5L_t$ downstream of the outlet header. All thermocouple signals ($T_{a,in}$, $T_{w,in}$, and $T_{w,out}$) were recorded at steady-state by a data acquisition system (Keysight 34972A).

2.5. Data processing

The thermal performance of a compact heat exchanger core is commonly reported in terms of the Nusselt number (Nu_x), which first requires determination of the air-side heat transfer coefficient (h_a). To obtain h_a, the measured variables ($T_{w,in}$, $T_{w,out}$, $T_{a,in}$, Q_a, and Q_w) were processed using the ϵ-NTU method.

The heat transferred out of the water-stream ($\dot{q}$) is given by:

$$\dot{q} = \dot{m}_w c_{p,w} (T_{w,in} - T_{w,out}) \tag{1}$$

where $\dot{m}_w$ is the mass flowrate of the water, $c_{p,w}$ is the specific heat capacity, $T_{w,in}$ and $T_{w,out}$ respectively represent the water temperatures at the inlet and outlet of the header tubes. The maximum theoretically achievable heat rate is:

$$\dot{q}_{max} = C_{min} (T_{w,in} - T_{a,in}) \tag{2}$$

where $C_{min} = \min(C_a, C_w)$ and $T_{a,in}$ is the temperature of the air entering the core. C_a and C_w are the specific heat rates of the air and water-streams, respectively defined as:

$$C_a = \dot{m}_a c_{p,a} = \rho_a Q_a c_{p,a} \tag{3}$$

$$C_w = \dot{m}_w c_{p,w} = \rho_w Q_w c_{p,w} \tag{4}$$

where $\dot{m}$, c_p, ρ, and Q respectively represent the mass flow rate, specific heat capacity, density, and volumetric flow rate; the subscripts a and w refer to the air and water-streams respectively. The effectiveness (ϵ) follows as:

$$\epsilon = \frac{\dot{q}}{\dot{q}_{max}} \tag{5}$$

from which the number of transfer units (NTU) for single pass cross flow conditions with both fluids unmixed can be solved iteratively using the explicit relation:

$$\epsilon = 1 - exp\left(\frac{NTU^{0.22}}{C_r}\{exp[-C_r(NTU)^{0.78}] - 1\}\right) \tag{6}$$

where

$$C_r = \frac{C_{min}}{C_{max}} = \frac{\min(C_a, C_w)}{\max(C_a, C_w)} \tag{7}$$

From the definition of NTU, one may calculate the overall heat transfer coefficient U based on the total air-side heat transfer surface area A_a, as:

$$U = \frac{C_{min} NTU}{A_a} \tag{8}$$

The air-side heat transfer coefficient h_a was then calculated using a one-dimensional steady-state surface energy balance, assuming negligible fouling resistance and constant thermo-physical properties:

$$h_a = \frac{1}{\eta_0}\left\{\frac{1}{U} - A_a R_{cond} - \frac{A_a}{A_w h_w}\right\}^{-1} \tag{9}$$

where η_o is the fin surface efficiency, R_{cond} is the conduction resistance of the tube wall, A_w is the inner surface area of the tube, and h_w is the water-side heat transfer coefficient. For the un-finned surfaces, $\eta_o = 1$ whereas for the louvered-fin surface η_o is given by

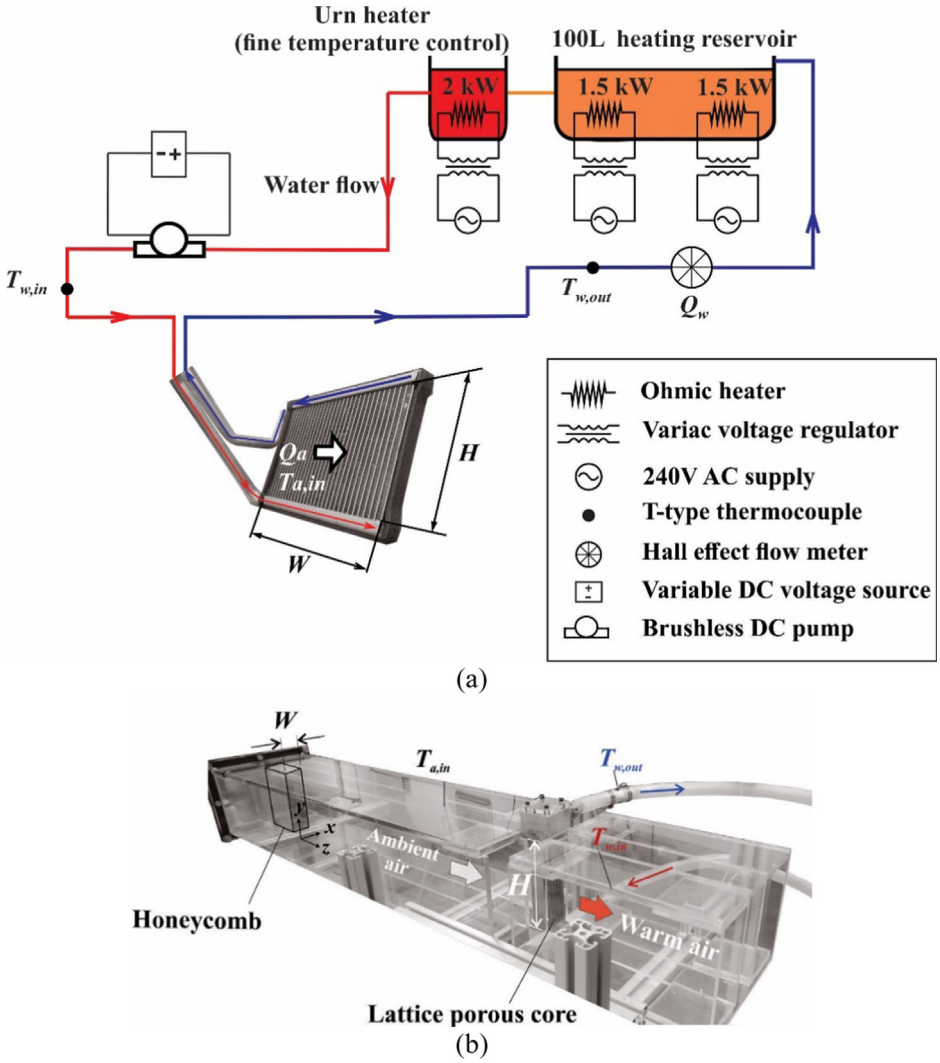

Fig. 3. Test setup: (a) Schematic showing supply of hot water through the header tubes of a test core with water temperature and flow measurement instruments, (b) Blowdown rectangular wind-tunnel showing the transverse (x), lateral (y), and longitudinal (z) directions for a lattice porous heater core positioned in the test section.

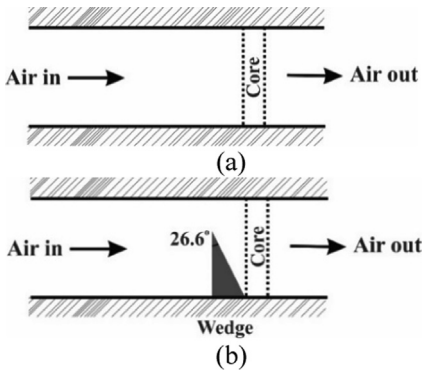

Fig. 4. Schematic of the wind tunnel test section: (a) With uniform stream i.e., at design conditions, (b) With non-uniform stream caused by a wedge i.e., at off-design conditions.

$$\eta_0 = 1 - \frac{A_f}{A_a}(1 - \eta_f) \tag{10}$$

where A_f is the total surface area of the fins. The fin efficiency η_f is given by:

$$\eta_f = \frac{\tanh(ml)}{ml} \tag{11}$$

where for a louvered fin geometry on the air-side [24],

$$m = \sqrt{\frac{2h_a}{k_{al}\delta}\left(1 + \frac{\delta}{L_f}\right)} \tag{12a}$$

and

$$l = \frac{(\sqrt{b^2 + P_f^2} - \delta)}{2} \tag{13a}$$

where k_{al} is the thermal conductivity of the fin material, δ is the fin thickness, L_f is the fin length in the flow direction, b is the fin height, and P_f is the fin pitch. For a cylindrical fin geometry on the air-side we have [25],

$$m = \sqrt{\frac{4h_a}{k_{al}D_l}} \tag{12b}$$

and

$$l = l_l + \frac{D_l}{4} \tag{13b}$$

where D_l is the fin ligament diameter and l_l is the fin ligament length.

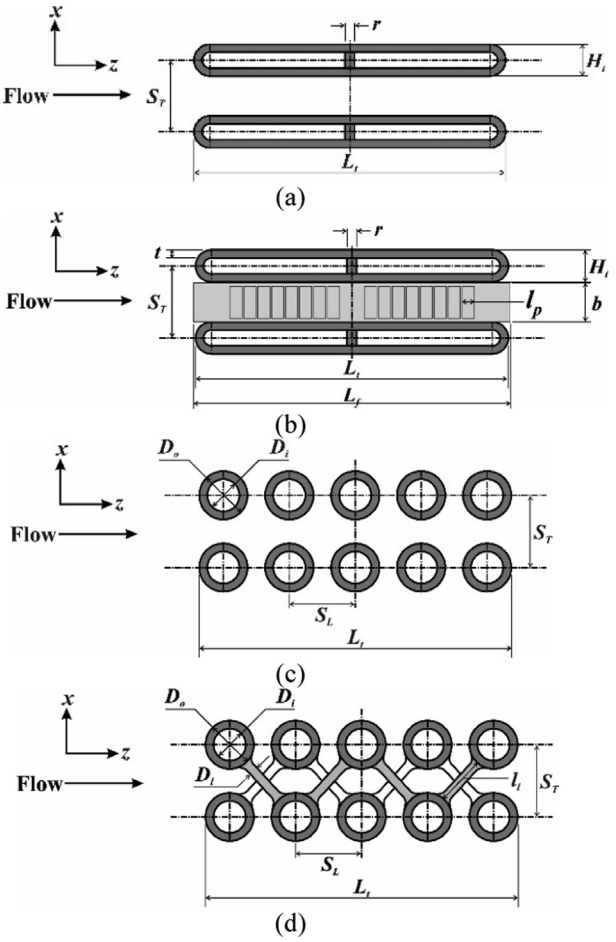

Fig. 5. Cut-away views showing core dimensions: (a) Flat tube array without fins, (b) Louvered fin-and-tube core, (c) Circular tube bank without fin ligaments, (d) Lattice porous core with staggered fin ligaments.

Table 1
Tubes and fin dimensions.

Component	Parameter	Value (± 0.01 mm/ ± 0.5°)
Louvered fin	L_f	27.00
	P_f	0.80
	S_1	1.85
	S_2	1.85
	l_p	0.93
	θ	30°
	δ	0.04
Flat tube	L_t	27.00
	S_T	7.25
	H_t	1.28
	t	0.40
	r	1.20
Circular ligament	D_l	1.00
	l_l	6.00
Circular tube	S_T	7.25
	S_L	6.00
	D_o	2.98
	D_i	2.14

The tube wall conduction resistance term is dependent on the tube geometry. For the flat tubes found in the louvered fin core, the wall conduction was approximated as that through a plane wall. Consequently,

$$R_{cond} = \frac{t}{k_{al}A_{wall}} \tag{14a}$$

where t is the tube thickness, k_{al} is the tube's thermal conductivity, and $A_{wall} = L \times L_t$. is the area of the flat surface of the tube. For the circular tubes found in the lattice porous core, the conduction resistance is given by:

$$R_{cond} = \frac{\ln\left(\frac{D_o}{D_i}\right)}{2\pi k_{al}L} \tag{14b}$$

where D_o, D_i, and L respectively represent the outer diameter, inner diameter, and the length of the tube.

For the water-side Nusselt number Nu_w of the high aspect ratio flat tubes, an analytical correlation which assumes laminar fully developed conditions, constant axial wall heat flux, and constant peripheral wall temperatures prevailing throughout the tube length was used [24]:

$$Nu_w = 8.235(1 - 2.0421\alpha^* + 3.0853\alpha^{*2} - 2.4765\alpha^{*3} + 1.0578\alpha^{*4} - 0.1861\alpha^{*5}) \tag{15a}$$

where

$$\alpha^* = \frac{H_t - 2t}{\frac{1}{2}(L_t - 2t - r)}$$

Here, H_t is the tube height, L_t the tube width, and r the center rib thickness. For circular tubes, the laminar fully developed solution was used [25]:

$$Nu_w = 4.36 \tag{15b}$$

The water-side heat transfer coefficient h_w can then be extracted using the definition of the Nusselt number:

$$h_w = \frac{k_w}{D_{h,t}}Nu_w \tag{16}$$

where k_w is the thermal conductivity of water and D_t is the internal hydraulic diameter of the tube.

Eqs. (9)–(13) were solved iteratively for the finned surfaces, starting with $\eta_o = 1$, and refining the heat transfer coefficient h_a until convergence of η_o was achieved to within 10^{-6}. Thereafter, the air-side Nusselt number Nu_x based on the characteristic length × was computed using the definition:

$$Nu_x = \frac{h_a x}{k_a} \tag{17}$$

where conventionally, $x = l_p$, or × $= D_o$, for a louvered fin core or a cylinder bank respectively. The hydraulic diameter of the wind tunnel D_h is often used as a characteristic length in this study and is defined as

$$D_h = \frac{4WH}{2(W + H)} \tag{18}$$

After calculating the Nusselt number, the air-side Colburn j-factor was computed based on a characteristic length × using the definition:

$$j_x = \frac{Nu_x}{Re_x Pr^{1/3}} \tag{19}$$

For conventional characteristic length scales, the Reynolds number Re_x was calculated using the maximum velocity through the core's minimum flow-facing cross-section, i.e., the bulk air flowrate Q_a divided by the free-flow area through the core, which is given by the difference between the total frontal core area (LW) and the projection of the flow-facing fins and tubes surface areas. Otherwise, when D_h was used as a length-scale, the average bulk velocity of the air-flow upstream of the core was used, i.e., the bulk flowrate Q_a divided by the tunnel area ($L \times W$).

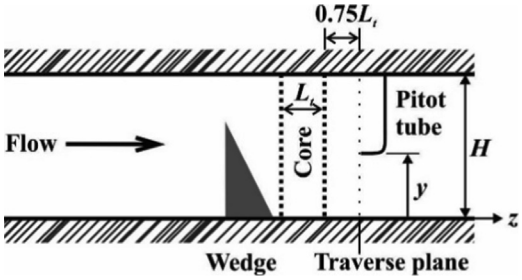

Fig. 6. Schematic of the wind-tunnel test section showing the downstream traverse plane for a Pitot tube.

2.6. Uncertainty analysis

If $y = f(x_1, x_2, \ldots, x_n)$ then the uncertainty propagated by x_i in the variable y is given by [26]:

$$\Delta y = \sqrt{\left(\frac{\partial y}{\partial x_1}\Delta x_1\right)^2 + \left(\frac{\partial y}{\partial x_2}\Delta x_2\right)^2 + \cdots + \left(\frac{\partial y}{\partial x_n}\Delta x_n\right)^2} \quad (20)$$

where Δx_i is the absolute uncertainty in x_i. Eq. (20) has been used to estimate the overall experimental uncertainties associated with the steady-state temperature and flowrate measurements. For the range of Reynolds numbers considered in this study, the maximum relative uncertainties were 13.0%, 2.5%, and 12.9% for the Nusselt numbers, Reynolds numbers, and Colburn j-factors respectively.

3. Discussion of results

3.1. Thermo-hydraulic characteristics of a louvered fin core under non-uniform flow

To determine the velocity distribution of the air-stream entering a core, a Pitot tube was traversed laterally (from $y = 0$ to $y = H$) along the mid-span of the wind-tunnel having a wedge upstream of an empty test section (i.e., without any core inserted). As shown in Fig. 7, the wedge blockage reduces the local flow area in the upper region ($0.6 \leq y/H \leq 1.0$), which results in local continuity-induced acceleration. Separation at the wedge apex is expected due to the sharp angle, which results in a slow-moving re-circulating flow in proximity with the lower region of the core, $0 \leq y/H \leq 0.6$. The dip in velocity at $y/H = 0.78$ followed by an increase and then gradual reduction in velocity as y/H decreases is characteristic of a shear layer ensuing the separation. The separation has been evidenced also by flow visualization in previous work [15].

When relatively high momentum fluid in the region $0.6 < y/H < 1.0$ encounters the louvered-fin core, a portion of fluid travels through the fin passages (of width P_f) to exit on the opposite side while aerodynamic resistance in the longitudinal (z) direction causes the remaining portion to turn downward (in the negative y-direction). Some of this remaining fluid is pushed through the fin passages (at a lower longitudinal velocity) on its way down towards the bottom wall of the wind-tunnel, but the rest either exits as a jet-like structure through a relatively wide opening found between the bottom-most fin and the header tube, as seen near $y/H = 0.03$, or gets entrained into the re-circulating flow.

Since the exit velocity profile remains non-uniform and of a similar shape to the inlet velocity profile, it can be concluded that the louvered fin structure provides certain resistance to flow in the lateral (y) direction. Downward dispersion of the high momentum fluid from the top region occurs only outside of the core structure, and any fluid making it through the lower region of the core is of relatively low velocity in the z-direction. As a result, the flow in the top region tends to transition from a louver-directed flow to a duct-directed flow, as illustrated in Fig. 8. The flow cannot traverse the lateral direction within the core because the deflection and turnaround louvers (i.e., S_1 and S_2 respectively; Fig. 2(c)) are known to direct incident air-streams along their lengths [14].

Steady-state temperature measurements on heated water passing through the louvered fin core were carried out to quantify the effect of the foregoing off-design configuration on heat transfer. A reference case to determine the credibility of the test setup was first established by placing a louvered fin-and-tube heater core in a uniform, unidirectional air-stream without any upstream or downstream obstructions (Fig. 4(a)). The setup conformed to the experimental conditions adopted by previous researchers [4,5,8]. Under these reference conditions, measurements were taken for the range of air-side Reynolds numbers based on louver pitch $140 \leq Re_{Lp} \leq 260$, which represents a central portion of the Reynolds number range typically encountered in an ACCS unit (i.e., $60 \leq Re_{Lp} \leq 360$). The variation of Colburn j-factor (j_{lp}) in this range is plotted against widely accepted correlations in Fig. 9(a). Achaichia & Cowell's [4] prediction is in line with the current data, with the maximum deviation being 16.7% while majority of the points lie within the reported correlation precision of 10%. The other correlation valid in this range [4] has a maximum deviation from the current data of up to 14.4%, which is within the reported correlation precision of 15%. Thus, the data are consistent with previous studies, implying that reliable comparisons can be made against these results within the specified range of Reynolds numbers.

The non-uniform incident stream caused by the wedge reduces the heat transfer performance of the louvered fin core by up to 20%, as shown in Fig. 9(b). This is due to the combined effects of (1) the sensitivity of louvered fins to the incoming velocity and (2) the limited capability of the louvered fins to laterally disperse the incoming flow. In areas of low velocity (e.g., $0.0 < y/H < 0.6$), the flow is largely duct-directed which reduces boundary layer periodicity over the fin surfaces. This compromises the wall shear stress and associated heat transfer. Therefore, only the upper area of the core ($0.6 < y/H < 1.0$) can be involved in significant heat transfer.

3.2. Lattice porous core concept and thermo-hydraulic performance

(a) Underlying mechanism: aerodynamic anisotropy

To overcome the heat transfer performance deterioration of a heater core under off-design conditions, such as those caused by the wedge in this study, it is firstly necessary that the core is insensitive to the incoming velocity's magnitude and angle. Hence, the intended heat transfer surfaces should have the same dominant mechanism for heat

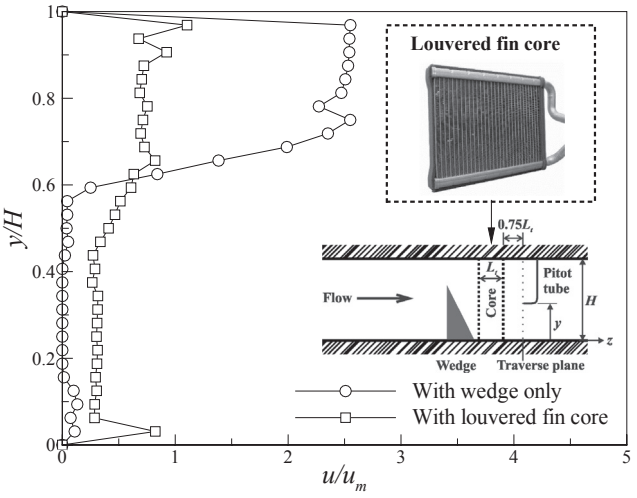

Fig. 7. Velocity profiles measured 0.75 L_t downstream of a louvered fin core with a wedge placed immediately upstream as indicated in the inset.

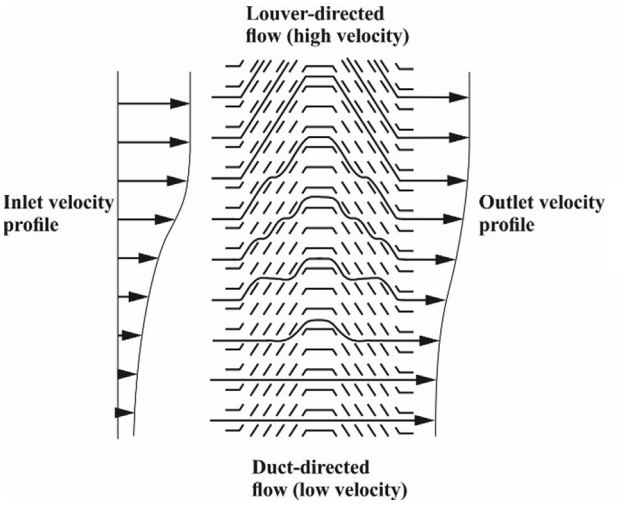

Fig. 8. Typical flow paths and exit velocity profile for louvered fins with non-uniform inlet velocity profile (adopted from Bellows [13]).

transfer over a wide range of Reynolds numbers, and should be geometrically isotropic to provide insensitivity to the flow angle. Secondly, it needs to be ensured that lateral hydraulic dispersion of the flow can be enabled within the core so that no portions of the core are short of sufficient coolant flux. Lastly, since the available pumping power of an ACCS unit is usually constrained by a vehicle's engine power, minimizing the pressure drop across the core is imperative

Porous materials are obvious candidates that meet the foregoing requirements. In addition to increasing heat transfer, Barnoon & Toghraie [27] and Arasteh et al. [28] showed that porous materials redistribute the velocity profile of an incident flow-stream, and the extent of re-distribution changes with porosity. Arasteh et al. [28] also showed that using multilayered porous materials allows one to control the shape of the velocity profile and the associated temperature gradients. A limiting factor, however, is the pressure drop across the porous medium. Therefore, a highly porous truss-like structure is sought in the current study.

A cylindrical extended surface has been shown to have aerodynamic anisotropy (i.e., directional dependence of the level of drag incurred by the incident stream) when arranged in a staggered bank [29]. Barratt & Kim [20] leveraged this property of staggered cylinder banks to effectively re-distribute an incidentally non-uniform fluid stream. Based on their concept, the non-uniform incident stream caused by the wedge would be dispersed laterally within the core if the relative aerodynamic resistance between the longitudinal (z) and lateral (y) directions were suitably tailored by changing the bank's porosity, as illustrated in Fig. 10. When lateral dispersion occurs within the core, the concentrated flow in the upper portion of the coolant channel will have a re-distributed velocity profile after passing through the core as illustrated in Fig. 10(a) and (b).

(b) Hydraulic dispersion characteristics

To realise an aerodynamically anisotropic heater core, a lattice porous core consisting of circular pin–fin ligaments running horizontally in the transverse (x) direction were attached to laterally (y-direction) running cylindrical tubes, as shown in Fig. 11. The core, manufactured by additive laser sintering, was placed inside the test section of the wind-tunnel having a wedge immediately upstream of it, and a Pitot tube was traversed downstream of the core. Fig. 12 shows that the lattice porous core with porosity of 0.71 could reverse the incident velocity profile caused by the wedge. When the high momentum fluid in the top region ($0.6 < y/H < 1.0$) encountered the core, the relatively higher aerodynamic resistance of the tube-bank cross-section in the longitudinal (z) direction forced the flow laterally, downward (in the negative y-direction), resulting in the re-distributed exit velocity profile. When the porosity of the core was increased to 0.79 by reducing the cylinder diameter while keeping the fin-functioning ligaments in the same locations, aerodynamic resistance in the longitudinal direction was reduced and resulted in a more uniform exit velocity profile.

(c) Thermal performance

With the wedge simulating the non-uniform off-design operation in the ACCS, a 20% decrease is noted for the louvered fin-and-tube core as shown in Fig. 13 where R represents a normalized performance ratio defined as:

$$R = \frac{Nu \;\; at \;\; off \;\; design \;\; conditions}{Nu \;\; at \;\; design \;\; conditions} \tag{21}$$

On the other hand, with the lattice porous heater core, a uniform-like exit velocity profile, due to hydraulic dispersion of the flow after the wedge, suggested that equal amounts of coolant streams contacted the core surface, which would ideally result in uniform cooling of the entire core. The steady-state heat transfer performance of the lattice porous core with porosity of 0.79 is plotted in Fig. 13(a). Under uniform flow (referred to as "design conditions" in this study), the lattice porous core performs thermally as good as the louvered fin core. A non-uniform incident air-stream (i.e., off-design conditions) conversely causes a

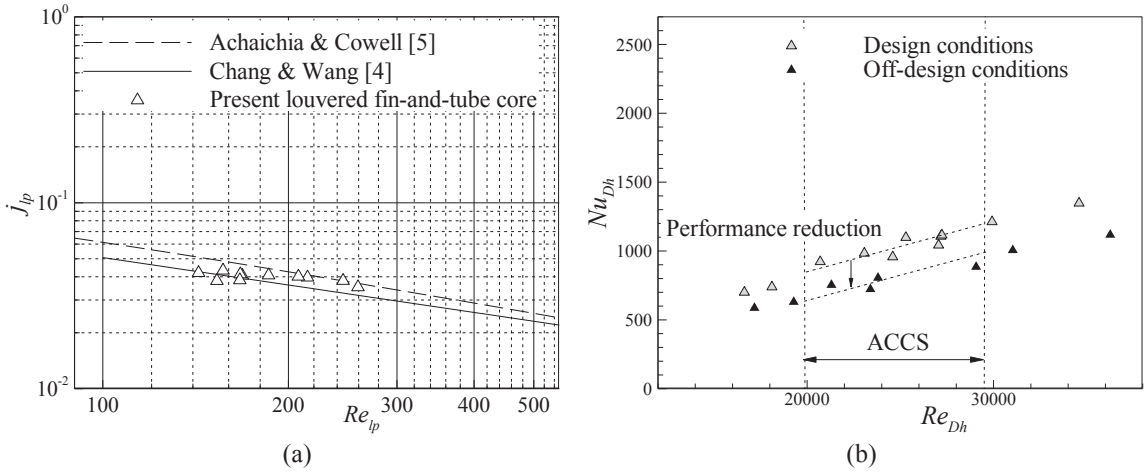

Fig. 9. Overall thermal performance: (a) Heat transfer performance of a louvered fin core at design conditions, (b) Heat transfer performance of a louvered fin core under uniform and non-uniform flow conditions.

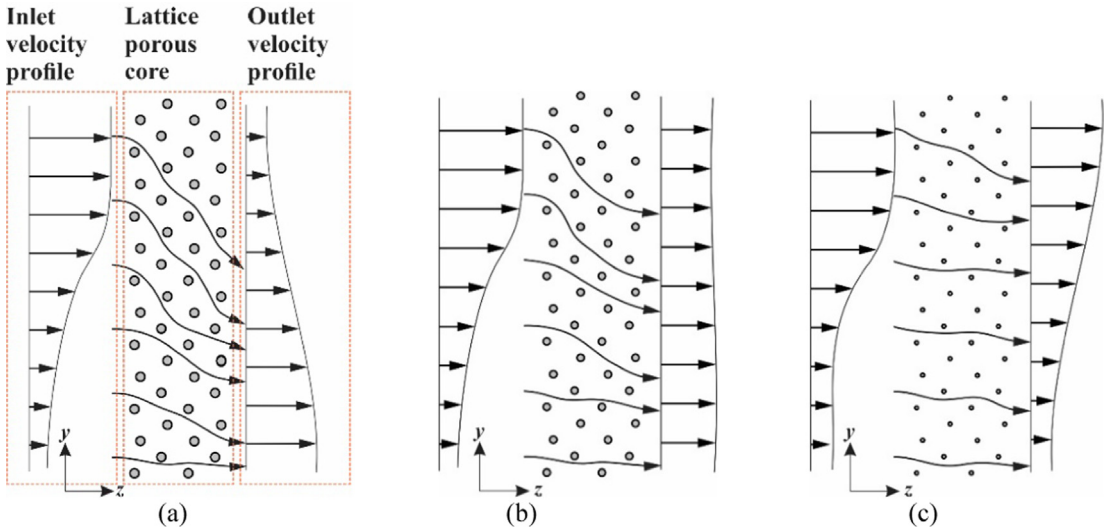

Fig. 10. Typical flow paths and velocity profiles for lattice porous cores with non-uniform incident velocity (adopted from Barratt & Kim [20]): (a) Low porosity & high lateral dispersion, (b) Critical porosity, (c) High porosity & low lateral dispersion.

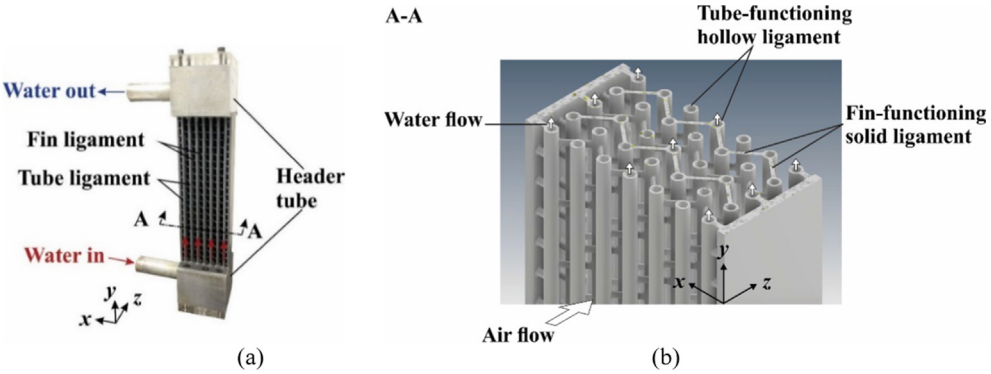

Fig. 11. Lattice porous heater core: (a) Assembled core with header tubes, (b) Cut-away view in the *x*-*z* plane (A-A).

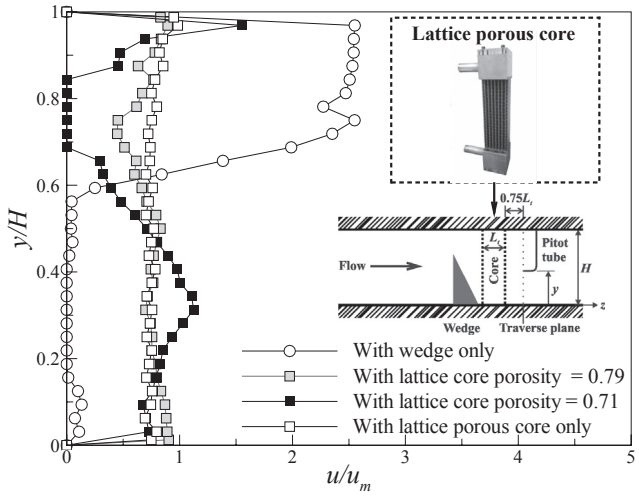

Fig. 12. Velocity profiles $0.75L_t$ downstream of a lattice porous heater core with a wedge placed immediately upstream as indicated in the inset.

13%~21% increase in heat transfer performance for the lattice porous core.

With a uniform incident air-stream, longitudinally (*z*) directed momentum in the lower region of the core ($0 < y/H < 0.6$) absorbs any laterally directed momenta by the lattice porous core. Furthermore, since the staggered bank is symmetric about the longitudinal (*z*) axis, equal amounts of *z*-directed momentum impinging the core surface would entail lateral momentum of similar magnitude in both positive and negative *y*-directions from the lower ($y/H < 0.5$) and upper ($y/H > 0.5$) core regions respectively (due to the closest end-wall), whose effects cancel on the macro-scale. Therefore, with the wedge placed upstream of the lattice porous core, a debilitated *z*-directed flux of coolant stream in the lower regions ($0 < y/H < 0.6$) enables hydraulic dispersion to be more pronounced as laterally directed momentum caused by the staggered bank is relatively less disturbed by the low-momentum longitudinal stream found in the lower region ($y/H < 0.6$). It follows that the dispersed flow-stream, traversing laterally through the core, inevitably impinges a larger number of fin-functioning ligaments before exiting the core (i.e., the flow follows a more tortuous path) compared to when the flow merely passes through the core purely longitudinally at design conditions. As a result, thermal dispersion – intensive flow mixing in the vortical wake structures behind the circular ligaments - within the core is augmented, which leads to higher overall heat transfer at off-design conditions [30]. A similar conclusion was also reached by Moradi et al. [31], where porous inserts in a double-pipe heat exchanger were seen to increase the heat transfer coefficient by up to 19%. It was reasoned that thermal dispersion (and therefore the heat transfer) was enhanced, due to an increase in the irregular and random motions of nano-particles within the MWCNT-water nanofluid.

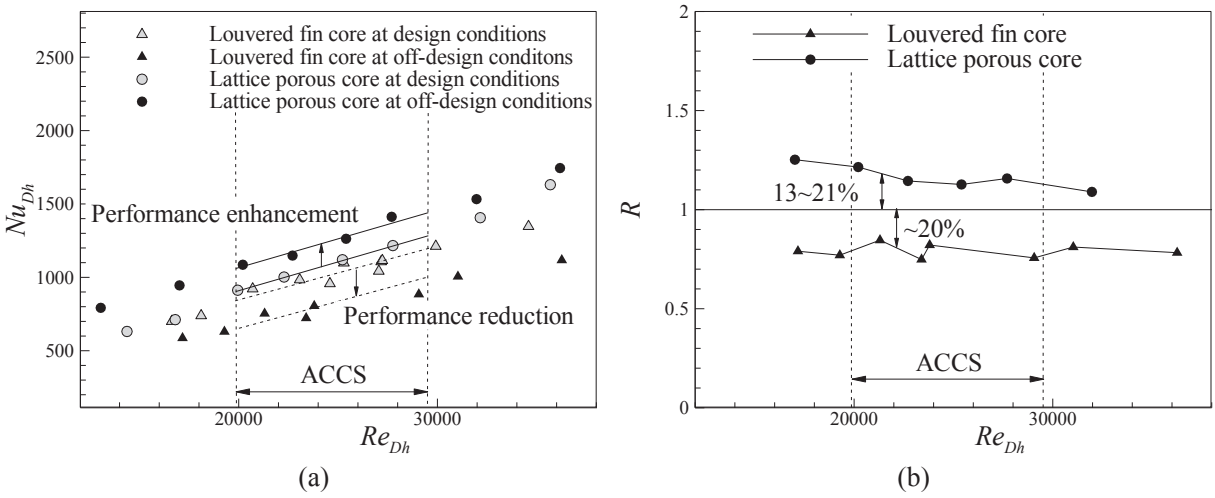

Fig. 13. Overall thermal performance: (a) Heat transfer performance of cores under uniform (design) and non-uniform (off-design) conditions, (b) Off-design heat transfer performance normalized by design performance.

3.3. Role of fins in thermal dispersion

It is of interest to quantify the effects of the circular fin-functioning ligaments on the overall heat transfer of the lattice porous core. For an inline tube bank, which represents the lattice porous core structure without any fin-functioning transverse ligaments, the heat transfer behaviour is not affected significantly by off-design conditions as shown in Fig. 14(a). Flow over the in-line circular tube bank used in this study is comparable with the correlation reported by Zukauskas [30], which characteristically shifts abruptly at $Re_D = 1000$ due to the growth and interaction of the wake region of a preceeding cylinder with the adjacent downstream cylinders. This causes a shift in the location of laminar to turbulent boundary layer transition over the fore surface of downstream cylinders, producing the observed shift in Nusselt number.

With the fin-functioning ligaments, the overall thermal performance of the lattice porous heater core is doubled within the range of ACCS unit flowrates when performing at design conditions as shown in Fig. 14(b). This is attributed to the increased heat transfer surface area and promoted thermal dispersion over the extended surface comprising a staggered cylinder bank. At off-design conditions, there is a further 13–21% enhancement of heat removal performance attributable to lateral hydraulic dispersion of the coolant-stream across the height (H) of the core. This results in extension of the coolant-stream's flow path through the core followed by increased interaction with fin-functioning ligaments before exiting the core. Therefore, with lateral hydraulic dispersion, the inclusion of the present fin-functioning ligaments is more advantageous under off-design conditions than under design conditions.

3.4. Summary

Louvered fins typically fail to disperse an incidentally non-uniform air-stream in certain directions, since the fin passages tend to restrict movement of air stream in these directions. Thus, a non-uniform incident air-stream is unable to reach all parts of a louvered fin-and-tube core with sufficient momentum to "activate" the louvers (i.e., to induce louver-directed flow) for heat transfer enhancement. The thermal performance of a louvered fin-and-tube heater core is therefore reduced when operating under non-uniform coolant flow-streams, which are typically found inside compact systems such as an ACCS unit. To overcome this thermal performance deterioration, associated with coolant flow-stream maldistribution, a lattice porous core can be used. This core allows the incident flow-stream to traverse through the lateral, transverse, and longitudinal directions within the core. The overall geometry and porosity of the core can be tuned to control the flow for different applications. For the specific case of an ACCS unit's flow conditions, the non-uniform incident velocity profile was redistributed within the core to produce a uniform-like flow-stream. Consequently,

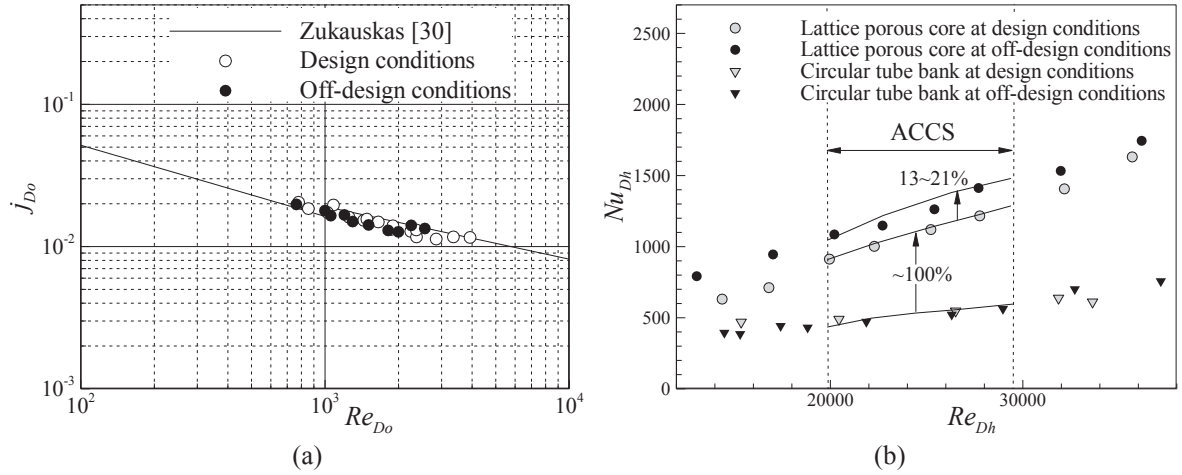

Fig. 14. Heat transfer in a lattice porous heater core: (a) Design/off-design heat transfer performance of a circular tube bank without horizontal fin-functioning ligaments, (b) Contribution of fins to the overall heat transfer in a lattice porous heater core.

the heat transfer performance was enhanced due to increased thermal dispersion within the core. The lattice porous core thermally performed better under a non-uniform incident flow-stream than under a uniform flow-stream. Thus, the need for upstream components to re-distribute the incident coolant stream was eliminated. This ensured that the compactness of the overall system is maintained while the core's thermal performance is significantly augmented.

4. Conclusions

The present study has demonstrated the thermo-fluidic characteristics of a newly developed lattice porous heater core for compact operations, relative to a conventional louvered fin-and-tube heater core. The lattice porous core was designed to mitigate highly localized cooling by non-uniform incident coolant streams which typically leads to the deterioration of designed heat transfer performance. The newly drawn conclusions are as follows. A physical obstruction characteristic of overall compactness of the system causes a non-uniform incident coolant stream, resulting in up to 20% thermal performance reduction relative to the designed thermal performance under uniform incident coolant streams. With the lattice porous heater core, conversely, up to 15% improvement in heat transfer was achieved due to enhanced lateral dispersion. Under the highly non-uniform incident coolant streams, the staggered arrangement of fin-functioning ligaments promotes lateral dispersion of momentum within the lattice core via aerodynamic anisotropy, which acts to increase the total heat transfer surface area. The present results conclusively show that although the deterioration of thermal performance of compact thermal systems (e.g., highly non-uniform incident coolant streams) is inevitable, such deteriorated thermal performance can be overcome by allowing the incident coolant stream to be laterally dispersed within the core.

The present work encompasses a proof of concept. Further considerations for future work include optimization of the lattice porous core geometry for maximum heat transfer, minimum pressure drop, and minimum noise production. Moreover, since the manufacturing method used in this study (i.e., laser sintering) is difficult and expensive, it would be worthwhile to explore other materials and methods more suitable for a commercial production line.

Declaration of Competing Interest

The authors declare that they have no known competing financial interests or personal relationships that could have appeared to influence the work reported in this paper.

Acknowledgements

This work was supported by the Open Fund of the State Key Laboratory of Mechanics and Control of Mechanical Structures (MCMS-I-0219K01 and MCMS-E-0219K02), China.

Appendix A. Supplementary material

Supplementary data to this article can be found online at https://doi.org/10.1016/j.applthermaleng.2020.115430.

References

[1] W.M. Kays, A.L. London, Compact Heat Exchangers, third ed., McGraw-Hill Inc., New York, 1964.
[2] A.M. Jacobi, R.K. Shah, Air-side flow and heat transfer in compact heat exchangers: A discussion of enhancement mechanisms, Heat Transfer Eng. 19 (4) (1998) 29–41.
[3] C.J. Davenport, Heat transfer and flow friction characteristics of louvred heat exchanger surfaces, in: J. Taborek, G.F. Hewitt, N. Afgan (Eds.), Heat Exchangers: Theory and Practice, Hemisphere/McGraw-Hill, New York, 1983, pp. 397–412.
[4] Y.J. Chang, C.C. Wang, A generalized heat transfer correlation for louver fin geometry, Int. J. Heat Mass Transf. 40 (3) (1997) 533–544.
[5] A. Achaichia, T.A. Cowell, Heat transfer and pressure drop characteristics of flat tube and louvered plate fin surfaces, Exp. Therm. Fluid Sci. 1 (1988) 147–157.
[6] M.H. Kim, C.W. Bullard, Air-side thermal hydraulic performance of multi-louvered fin aluminium heat exchangers, Int. J. Refrig. 25 (2002) 390–400.
[7] J. Dong, J. Chen, Z. Chen, W. Zhang, Y. Zhou, Heat transfer and pressure drop correlations for the multi-louvered fin compact heat exchangers, Energy Convers. Manage. 48 (2007) 1506–1515.
[8] P. Shinde, C. Lin, A heat transfer and friction factor correlation for low air-side Reynolds number applications of compact heat exchangers Science and Technology for the, Built. Environ. 23 (2017) 192–210.
[9] R.L. Webb, P. Trauger, Flow structure in the louvered fin heat exchanger geometry, Exp. Therm. Fluid Sci. 4 (1991) 205–217.
[10] C. T'Joen, M. De Paepe, F. Vanhee, Heat exchanger behaviour in non uniform flow, Exp. Heat Transfer 19 (4) (2006) 281–296.
[11] S.P. Datta, P.K. Das, S. Mukhopadhyay, Obstructed airflow through the condenser of an automotive air conditioner - Effects on the condenser and overall performance of the system, Appl. Therm. Eng. 70 (2014) 925–934.
[12] P. Blecich, Experimental investigation of the effects of airflow nonuniformity on performance of a fin-and-tube heat exchanger, Int. J. Refrig. 59 (2015) 65–74.
[13] K.D. Bellows, Flow Visualization of Louvered-Fin Heat Exchangers, Thesis, The Air Conditioning and Refrigeration Center, University of Illinois, Urbana, IL, 1997.
[14] N.C. DeJong, A.M. Jacobi, Localized flow and heat transfer interactions in louvered-fin arrays, Int. J. Heat Mass Transf. 46 (2003) 443–455.
[15] T.I. Bhaiyat, S. Scheckman, H.Y. Lim, Y.H. Jeon, T. Kim, Off-design performance of a louvered fin-tube heater core in an automotive climate control system, Appl. Therm. Eng. 161 (2019) 114155.
[16] J.B. Kitto, J.M. Robertson, Effects of maldistribution of flow on heat transfer equipment performance, Heat Transfer Eng. 10 (1) (1989) 18–25.
[17] L. Henriksson, Performance of Compact Heat Exchanger in Non-Perpendicular Cooling Airflows, Thesis, Chalmers University of Technology, Gothenburg, 2015.
[18] D. Barratt, T. Kim, Diffuser, Johannesburg Patent WO/2015/049647, 2015.
[19] C.E. Kusuda, C.S. Roper, W. Vannice, A. Muley, K.J. Maloney, Micro-Lattice Cross-Flow Heat Exchangers for Aircraft, Canada Patent CA2836709, 2017.
[20] D. Barratt, T. Kim, A banked wide-angle diffuser with application to electrostatic precipitators, J. Power Energy 229 (2014) 88–98.
[21] Hanon Systems, What is Climate Control?, http://www.hanonsystems.com/En/Technology/WhatisClimate#what_tit4, 2019 (accessed 18 January, 2020).
[22] P.R. Shinde, Investigation of Low Reynolds Number Flow and Heat Transfer of Louvered Surfaces, Thesis, FIU Electronic Theses and Dissertations, Miami, 2016.
[23] M.H. Kim, B. Youn, C.W. Bullard, Effect of inclination angle on the air-side performance of a brazed aluminium heat exchanger under dry and wet conditions, Int. J. Heat Mass Transf. 44 (2001) 4613–4623.
[24] R.K. Shah, D.P. Sekulic, Fundamentals of Heat Exchanger Design, John Wiley & Sons Inc, Hoboken, 2003.
[25] F.P. Incropera, D.P. Dewitt, T.L. Bergman, A.S. Lavine, Fundamentals of Heat and Mass Transfer, sixth ed., John Wiley & Sons Inc., Hoboken, 2007.
[26] H.W. Coleman, W.G. Steele, Experimentation, Validation, and Uncertainty Analysis for Engineers, third ed., John Wiley & Sons Inc., Hoboken, 2009.
[27] P. Barnoon, D. Toghraie, Numerical investigation of laminar flow and heat transfer of non-Newtonian nanofluid within a porous medium, Powder Technol. 325 (2018) 78–91.
[28] H. Arasteh, R. Mashayekhi, D. Toghraie, A. Karimipour, M. Bahiraei, A. Rahbari, Optimal arrangements of a heat sink partially filled with multilayered porous media employing hybrid nanofluid, J. Therm. Anal. Calorim. 137 (2019) 1045–1058.
[29] T. Kim, T.J. Lu, Pressure drop through anisotropic porous mediumlike cylinder bundles in turbulent flow regime, J. Fluids Eng. 130 (2008) 104501.
[30] A. Zukauskas, Heat transfer from tubes in crossflow, Adv. Heat Transfer 18 (1987) 87–159.
[31] A. Moradi, D. Toghraie, A.H.M. Isfahani, A. Hosseinian, An experimental study on MWCNT–water nanofluids flow and heat transfer in double-pipe heat exchanger using porous media, J. Therm. Anal. Calorim. 137 (2019) 1797–1807.